Japan Geoscience Union Meeting 2015
(May 24th - 28th at Makuhari, Chiba, Japan)

SSS27-01 Room:103 Time:May 24 10:00-10:15

Statistical investigation of spatio-temporal densities of foreshocks to understand earthquake predictability

KAMOGAWA, Masashi[1*] ; TANAKA, Rika[1] ; ORIHARA, Yoshiaki[1] ; HASHIMOTO, Satoshi[1]

[1]Dpt. of Phys., Tokyo Gakugei Univ.

The relation between the size of earthquake preparation zone and the magnitude of forthcoming earthquake is different between nucleation and domino-like cascade models. The former model indicates that the magnitude is predictable before the mainshock of the earthquake, because the preparation zone is proportional to the rupture area. One the other hand, the latter indicates that the magnitude is unpredictable, because the rupture consisting of sequence of tiny earthquakes is unknown to terminate. Since this issue is still controversial, we would like to verify the two models using the methodology proposed by Lippiello et al. (Scientific reports, 2012). In the analysis, spatial occurrence rates of the foreshock and the aftershock are statistically compared. The results show that both the rates are similar and the distribution of the rates versus the epicentral distance depends on the magnitude of the mainshock. From the interpretation of these results, the nucleation model seems reliable.

Keywords: Earthquake, Foreshock, Mainshock

Japan Geoscience Union Meeting 2015
(May 24th - 28th at Makuhari, Chiba, Japan)

SSS27-02 Room:103 Time:May 24 10:15-10:30

Proper scoring systems available for probability forecasts targeting rare phenomena

HAYASHI, Yutaka[1*]

[1]Meteorological Research Institute

Necessary conditions for ensuring that newly introduced method can improve forecast are, existing *proper* scoring system and that the new method marks better score than the present method do. Murphy and Epstein (1967) pointed out that "all proper scoring system should encourage the meteorologists to make his probabilities correspond with his true belief." Probability Score (Brier, 1950; hereinafter called BS), which is well used for evaluating such as probability of precipitation forecasts, satisfies the mathematical term of the *proper* scoring rule; but, information gain (Kullback and Leibler, 1951) does not. The effort to score high in an *improper* scoring rule does not mean honest activity aiming for a better forecast in general, because the rule do not ensure forecasters to get the highest score in case they make forecast with their true belief. Therefore, we should become very careful about interpretation of the measurement or comparison of the forecast based on various information criteria and other *improper* scoring rule, although they still are very widely performed especially in the field of earthquake prediction study.

BS is defined as the expectation of the mean square error between forecasted probability and the existence or non-existence of intended phenomenon. The existence and non-existence are equally weighted. On the other hand, the users tend to give importance to the forecasts of relatively high probability and the cases of the existence, if the intended phenomena of the forecast is rare. Proper scoring systems available for probability forecasts targeting rare phenomena like large earthquakes are discussed below.

Proper scoring rule have to satisfy $E_s(x,c)=pS_1(x,c)+(1-p)S_0(x,c)$ (eq.1), and $E_s(p,c)>E_s(x,c)$ for all $x \neq p$ (eq.2), where p, f, i, c, S_i, and E_s are probability based on true faith by a forecaster, forecasted value, existence (0) or non-existence (1), benchmark forecast such as a probability based on basic statistics, score, and expected score, respectively. The rule also have to satisfy fair condition from the viewpoints to give higher score for more difficult issue to forecast, *i.e.* $S_0(c,f) \equiv S_1(1-c,1-f)$ (eq.3), and $\partial S_1/\partial f|_{c=const}>=0$, $\partial S_1/\partial c|_{f=const}<=0$ (eq.4).

The solutions of eq.1 and eq.3 satisfies $S_1(f,c)=-(i-f)B'(f,c)+(i-x)B'(x,c)-B(f,c)+B(x,c)$, $A=d^2B/df^2$ (eq.5), where A is any function.

A proper scoring system with suitable characteristics can be obtained after solving eq.5 in a certain boundary conditions and A, and if S_i satisfies eq.2 and 4.

For the first example, from the conditions about scores of benchmark forecast $S_i(c,c) \equiv 0$, score of perfect forecast $S_i(i,c) \equiv 1$, A=-2 and $S_i(f)=1-(i-f)^2$ (eq.6) are derived. $1-S_i(f)$ is BS.

For the other example, by using the boundary condition for expected score of the perfect forecast (f=i) $E_{s,p} \equiv 1$ instead, and assume that A is the expression of degree 0 of f, A=-2/c(1-c) and $S_i(f,c)=\{(i-c)\hat{}2-(i-f)\hat{}2\}/c(1-c)$ (eq.7) are derived. The fact $(1-S_i(f))/4$ is equivalent to BS in case of c=1/2 shows that eq.7 can be interpreted as an extended form of Brier's Score.

General solution for proper scoring systems, and particular solutions, so-called extended Brier's Score, available for probability forecasts targeting rare phenomena like large earthquakes are mathematically derived as I discuss above.

In the meeting, the author would like to introduce the details of derivation of equations and to discuss on the problem for the practical application of the scoring systems. Besides, mathematical solutions of proper scoring rules for warnings, which is a kind of binary forecast, has already been discussed based on expected-utility theory (Hayashi, 2014, JpGU).

Keywords: benchmark forecast, earthquake prediction, extended Brier's score, information gain, probability forecst, proper scoring rule

Japan Geoscience Union Meeting 2015
(May 24th - 28th at Makuhari, Chiba, Japan)

SSS27-03 Room:103 Time:May 24 10:30-10:45

Physical interpretation and detection of anomalies associated with crustal processes leading to large earthquakes

SUYEHIRO, Kiyoshi[1*] ; SACKS, Selwyn[2] ; TAKANAMI, Tetsuo[2] ; RYDELEK, Paul[2] ; SMITH, Deborah[2] ; HATANO, Takahiro[3]

[1]Japan Agency for Marine-Earth Science and Technology, [2]Carnegie Institution of Washington, [3]Earthquake Research Institute, University of Tokyo

Based on a cellular automata earthquake model proposed by Sacks and Rydelek (1995), we propose an observational approach to the problem of earthquake prediction (short-term). This approach is different from the detection of pre-seismic slip. We propose to revisit the dilatancy model. Previously reported magnitude dependent seismic quiescence (e.g. 1982 Urakawa-OKi earthquake, 1994 Northridge earthquake, 2008 Wenchuan earthquake) can be interpreted as a manifestation of the dilatancy hardening process. By incorporating this process, our model explains the magnitude selectivity. This information may be useful for raising awareness. We note that this phenomenon is not confined to the eventual earthquake zone but covers much wider area. If we advance this line of thinking, dilatancy breakdown can be expected before the eventual large faulting, which should result in fluid diffusion into cracks opened by dilatancy. Mature faults are known to have high permeability and may act to accelerate the process and lead to observable anomalies. Our model needs to include this phase to provide quantitative direction for detection. We propose that the observation of vertical strain will complement the existing multiple-parameter observations to provide useful data related to fluid distribution changes as a short-term precursor.

Keywords: seismic quiescence, dilatancy, cellular automata earthquake model

Japan Geoscience Union Meeting 2015
(May 24th - 28th at Makuhari, Chiba, Japan)

SSS27-04 Room:103 Time:May 24 11:00-11:15

Predicting changing rates of swarm activity by volumetric strain

KUMAZAWA, Takao[1*] ; OGATA, Yosihiko[1] ; KIMURA, Kazuhiro[2] ; MAEDA, Kenji[2] ; KOBAYASHI, Akio[2]

[1]The Institute of Statistical Mathematicsa, [2]Meteorological Research Institute

Near the eastern coast of Izu peninsula is an active submarine volcanic region in Japan, where magma intrusions have been observed many times. The forecast of earthquake swarm activities and eruptions are serious concern particularly in nearby hot spring resort areas. It is well known that temporal durations of the swarm activities have been correlated with early volumetric strain changes at a certain observation station of about 20 km distance apart. Therefore the Earthquake Research Committee (2010) investigated some empirical statistical relations to predict sizes of the swarm activity. Here we looked at the background seismicity rate changes during these swarm periods using the non-stationary ETAS model (Kumazawa and Ogata, 2013, 2014), and have found the followings. The modified volumetric strain data, by removing the effect of earth tides, precipitation and coseismic jumps, have significantly higher cross-correlations to the estimated background rates of the ETAS model than to the swarm rate-changes. Specifically, the background seismicity rate synchronizes clearer to the strain change by the lags around a half day. These relations suggest an enhanced prediction of earthquakes in this region using volumetric strain measurements. Hence we propose an extended ETAS model where the background rate is modulated by the volumetric strain data. Here we have also found that the response function to the strain data can be exponential functions with the same decay rate, but that their intersects are inversely proportional to distances between the volumetric strain-meter and the onset location of the swarm. Our numerical results by the same proposed model show consistent outcomes for the various major swarms in this region.

Keywords: nonstationary ETAS model, background seismicity, swarm, volumetric strain, prediction

Japan Geoscience Union Meeting 2015
(May 24th - 28th at Makuhari, Chiba, Japan)

SSS27-05 Room:103 Time:May 24 11:15-11:30

Seismo-ionospheric precursor monitoring system based on near-real-time spaceborne and ground GPS observation

TSAI, Ho-fang[1*] ; LIU, Jann-yenq[2] ; CHEN, Chia-hung[1] ; SUN, Yang-yi[2] ; HO, Tiffany[3]

[1]Department of Earth Sciences, National Cheng Kung University, Tainan, Taiwan, [2]Institute of Space Science, National Central University, Jhongli City, Taiwan, [3]Taiwan Analysis Center for COSMIC, Central Weather Bureau, Taipei, Taiwan

Recently, the global ionosphere map (GIM) has been used to study the seismo-ionospheric precursors (SIPs) intensively. In order to shorten the data latency, an SIP monitoring system is built up based on the near-real-time GIM processing. The GIM data is derived from the combination of the ground-based and spaceborne total electron content (TEC) observation by means of the spherical harmonic function, where the data is retrieved from a global GPS observational network and the FORMOSAT-3/COSMIC radio-occultation (RO) experiments. The temporal statistical analysis is developed to detect the SIPs at several important metropolitans such as Tokyo. Some new finding and results are to be further discussed. The spatial analysis will be introduced to finding the repeat, duration and distribution of worldwide SIPs to estimate the possibility of forthcoming large earthquakes in the future.

Keywords: global ionosphere map, seismo-ionospheric precursor, total electron content

Japan Geoscience Union Meeting 2015
(May 24th - 28th at Makuhari, Chiba, Japan)

SSS27-06 Room:103 Time:May 24 11:30-11:45

Long-term groundwater temperature change at a hot spring preceding the 2014 Nagano-ken Hokubu earthquake of M6.7

TSUKUDA, Tameshige[1*]

[1]None

On November 22, 2014, an large earthquake of M6.7 took place at the Kamishiro fault in Hakuba Village in the northern Fossa Magna region, central Japan. The Hakuba earthquake was predicted in a long-term basis: a historical earthquake, the Kamishiro active fault, accumulation of crustal strains, etc(Association for the Development of Earthquake Prediction, 1990). To clarify how large earthquakes are generated, we should closely observe changing signals associated with their preparatory process underground. For the purpose of monitoring the preparation process of large earthquakes, various kinds of surveys and nearby observations have been being conducted in the Hakuba Village region around the northern Fossa Magna. Affiliated organizations are Shinshu University, Toyama University, Tokyo Metropolitan University, Tokai University, Nagasaki University, and others. Among them, the observation of water temperature has been conducted at a hot located just west of the Kamishiro fault, since October 1998. The temperature has been slightly decreasing with a rate -0.17 degree/year before around 2009, whereas the rate grew more than before during recent five years as -1.5 degree/year, indicating that dilatation processes in the subsiding region on the footwall side of the fault had been going on before the earthquake.

Keywords: the 2014 Nagano-ken Hokubu earthquake of M6.7, earthquake prediction, precursor, water temperature, dilatation, contraction

Japan Geoscience Union Meeting 2015
(May 24th - 28th at Makuhari, Chiba, Japan)

SSS27-07 Room:103 Time:May 24 11:45-12:00

Empirical forecast of mainshocks based on foreshock activities - Application to the north-central Nagano prefecture -

MAEDA, Kenji[1*] ; HIROSE, Fuyuki[1]

[1]Meteorological Research Institute

1. Introduction

An earthquake with magnitude (M) 6.7 occurred on November 22nd, 2014 in the northern Nagano prefecture and it caused many injuries and housing damages. According to JMA, about four days before the mainshock, a pronounced foreshock activity that includes more than 40 small earthquakes with M less than 3.0, had been observed at the very near location of the mainshock. However, it is quite difficult to distinguish foreshocks from background seismicity before a mainshock occurs because we have not yet elucidated the physical process that associates foreshocks with a mainshock. Even though the situation is not easy, empirical approach is one of the realistic ways to use foreshock activity as a precursor of a mainshock. We have been investigating probabilistic features of empirically defined foreshocks and searching for the best parameters to define foreshocks which present relatively high performance to predict large earthquakes. Maeda (1996) and Maeda and Hirose (2012, 2014) proposed a foreshock definition which gives the highest performance to predict large earthquakes along the Japan trench and the Izu region. In this study we basically apply the same method to the seismicity in the north-central Nagano prefecture where foreshock activities are relatively higher than those in other inland regions of Japan. Then we estimate the best parameters to define foreshocks which give good performance of predicting mainshocks in the region.

2. Method

The method to search for parameters for foreshocks that present high prediction performance consists of four steps. 1) To eliminate small aftershocks from the original data. 2) To define foreshock candidates satisfying the condition that the number of Nf earthquakes with magnitude >= Mf occur during the period of Tf days in the segment of the size of D x D degree (latitude x longitude). 3) To set the alarm period of Ta days during which a mainshock is expected to occur after a foreshock candidate is found. 4) To search for the values of D, Mf, Tf, Nf and Ta which give high prediction performance by the grid search method. The prediction performance is measured mainly by dAIC that is defined as the difference of AIC for a stationary Poisson model and a model based on a foreshock activity, and additionally by alarm rate (AR: the fraction of mainshocks alarmed), truth rate (TR: the fraction of foreshock candidates followed by a mainshock), and probability gain (PG: the ratio of mainshock occurrence rate in the predicted space-time to background occurrence rate).

3. Data and Results

By applying the above method to the earthquakes with M >= 1.0 and depth <= 30 km cataloged by JMA during the period from 1998 through 2014 in the north-central Nagano region (35.6N-37.1N, 137.2E-139.0E), we obtained the best parameters for foreshocks as D=0.1 degree, Mf=2.0, Tf=1 day, Nf=5, and Ta=5 days to predict mainshocks with M>=5.0 among 45000 combinations of parameters of D(0.1, 0.2, 0.3), Mf(1, 1.5, 2, 2.5, 3), Tf(1, 2, 3, 5, 10), Nf(1, 2,...,20), and Ta(1, 2,...,30). The prediction performance is expressed as dAIC=66, AR=45% (=5/11), TR=12% (=8/69), and PG=333. If we use these parameters to define foreshocks, the 2014 Nagano earthquake mentioned at the opening sentence comes to be predicted by the foreshocks. Therefore we can say that a seismic activity such that observed about four days before the 2014 Nagano mainshock would be followed by a mainshock of M>=5.0 with about 12 % possibility, and to the contrary a mainshock with M>=5.0 would be preceded by a foreshock activity such that observed before the 2014 Nagano mainshock with about 45 % possibility. The value 12 % of TR is relatively low if compared with that for the specific region in the Japan trench (TR=30%) and for the Izu region (TR=23%) where we know the prediction performance is considerably high. This suggests that the prediction performance based on foreshock activities is largely different among regions.

Keywords: earthquake prediction, performance, foreshocks, Nagano prefecture, statistics, empirical relation

Japan Geoscience Union Meeting 2015
(May 24th - 28th at Makuhari, Chiba, Japan)

SSS27-08 Room:103 Time:May 24 12:00-12:15

Estimation of inelastic displacement of a fault zone during an earthquake cycle

YAMAMOTO, Kiyohiko[1*]

[1]none

1. Introduction: A damage zone/asperity model of faults was proposed to interpret the source parameters of an earthquake in terms of the physical properties of a fault zone (Yamamoto & Yabe, 2003, 2006 in SSJ meeting). In this model, the apparent fracture energy was calculated by assuming the complete elastic behavior of asperities in fracturing process. Further, the displacement vertical to a fault surface, which is produced by rotation of the damage zone, was calculated by first-order approximation. This approximation was found to cause an over-estimation of the apparent fracture energy. Here, the vertical displacement has been re-calculated by a more exact manner, taking account of inelastic displacement of asperities. Based on the results, the total slip accompanying an earthquake at plate boundary and the relationship between magnitude and recurrence time is examined.

2. A damage zone/asperity model: In this model, a fault zone means the damage zone including asperities. The fault surfaces are the boundaries between the fault zone and the host rocks outside of the fault zone. An asperity fractures at the time that the relative displacement between the surfaces reaches to $u*_c$, $u*_c=u_c+u_{fc}$ = $t(e_c+e_{fc})$, Here u_c and u_{fc}, respectively, are elastic and inelastic components of $u*_c$. t denotes the thickness of the fault zone. The displacements respectively correspond to the strains e_c and e_{fc}. u_c is called the critical displacement. After an asperity has fractured, the displacement between the fault surfaces is newly produced by u_b, which generates seismic waves. The fracturing produces the slip plane in the fault zone. The displacement on the slip plane is expressed by u_c+u_b. This means that the displacement seismological estimated is not equal to the displacement on the slip plane.

The vertical displacement v is produced by rotation of the damage zone accompanying slip-plane propagation. The vertical displacement acts against the normal stress on the fault plane. The apparent fracture energy is almost equal to the work of v acting against the normal stress. The density of the work per unit area w is written by $w=(s_n v)\}\approx s_n(1+2a)e_c u_c/2$, where s_n is the normal stress, and a is the ratio of e_{fc}/e_c. Assuming that s_n is equal to the litho-static pressure and the rigidity of asperities is 30GPa, $e_c\approx0.01$ is estimated for the depths from 10 to 20 km. For $e_c=0.01$, it is found that the data of apparent fracture energy versus critical displacement summarized by Ohnaka and Matsu ura (2002) are almost explained for (1+2a)/2?1. This means that the inelastic strain amounts 1/2 of elastic strain at the fracture of an asperity.

3. The recurrence of large earthquakes at plate-boundaries: Two large earthquakes are known to have occurred in the regions along the Sagami Trough. One is the 1703 Genroku earthquake and the other is the 1923 Kanto earthquake (Mw 8.0). The magnitude of the 1703 earthquake ranges from 7.9 to 8.5 depending on researchers. The displacement and the critical displacement of the 1923 earthquake are estimated at about 5.1m and 2.56 m, respectively. The convergence rate of inter seismic period is obtained as about 11.6 mm/year. This estimation is carried out on the assumption that asperities are elastic. Here, the deformation of an asperity, no matter how small asperity, is assumed to contain inelastic component of 0.5 times of the elastic deformation at fracturing. In this assumption, the total rate is 17.4 mm/year. This is almost equal to the inter-seismic slip rate along the Sagami trough presented by Loveless, J.P. and Meade, B.J. (2010).

If this rate of 11.6mm/year is constant at the plate boundary, the potential magnitude of an earthquake, of which recurrence time is 400 years, is estimated at about M8.5. The fault length is about 288 km. This length is almost equal to the length of the Sagani trough.

Keywords: damage zone/asperity model, inelastic displacement, fracture energy, critical displacement, 1923 kanto earthquake, plate boundary

Japan Geoscience Union Meeting 2015
(May 24th - 28th at Makuhari, Chiba, Japan)

SSS27-09 Room:103 Time:May 24 12:15-12:30

Euler Rotation of Focal Mechanism to determine the main shock of the East Japan Super Earthquake, March 2011

NIITSUMA, Nobuaki[1*]

[1]Institute of Geosciences, Shizuoka University, Sendai

Focal mechanism is most important information on the stress field. The focal mechanism is presented by the azimuth and dip of the princepal axes, P, T and N. The changes in the focal mechanism with the 6 parameters can be described by Euler pole and rotation, because the angular distances between pricepal axes are constantly 90^o (http://www.niitsuma-geolab.net/ Special Report 4).

CMT focal mechanism by Japan Meteorological Agency for the earthquakes in the main shock area of 2011 East Japan Super Earthquake are using for this analysis.

The Euler pole and rotation angle can be calculated for the three pairs of princepal axes, PT, TN and NP, on two earthquakes under the adjustment of the hand system. The calculated three Euler poles and rotation angles do not completely agree, because the azimuth and dip of princepal axes are presented with degree unit. Because the rotation angles around the Euler pole should same for the used pair of the princepal axes, the Euler pole is selected with the minimum difference in the rotation angles for the used pair of the princepal axes. The selected minimum differences are generally within 0.1^o.

The Euler rotation analysis is calculated from the main shock of East Japan Super Earthquake to the other earthquakes in this study. In the case of the position of the Euler pole locates on the southern side of the perpendicular line to the trench axis, the top of coordination system for princepal axes rotates toward island arc, and locates on the northern side, rotates toward trench. The rotation angle around Euler pole is defined with sign, positive toward island arc and negative toward trench.

All of 18 fore shocks, started by 16 February 2011, have positive rotation angles within 25^o. All of 35 after shocks have negative rotation angles smaller than -25^o. The complete separation of the sign of Euler rotations demonstrates that the Euler rotation of focal mechanism can be used for determination of main shock.

The positive rotation of fore shocks and the negative rotion of after shocks can be explained as follow. The stress field on the plate boundary along the Japan Trench is controlled by a resultant of shear stress and normal stress along the plate boundary and the compressional principal P axis dips toward trench. Fore shocks occurs by less fracture stress with less normal stress which has shallower dip of P axis than the main shock (36^o). After shocks occurs in the stess field controlled by mainly lithostatic stress with vertical P axis without shear stress which is released by the main shock.

The maximum fore shock M7.3 of 9 March 2011 with $+2.0^o$ of Euler rotation angle induced disorder by misjudgement as main shock, but the Euler rotation quantitically indicate to be fore shock and 7 earthquakes M5.2-6.8 in the next day 10 March 2011 had also positive rotation within $+25^o$.

Keywords: Euler pole, rotation angle, focal mechanism, hand system, determination of main shock, East Japan Super Earthquake

Japan Geoscience Union Meeting 2015
(May 24th - 28th at Makuhari, Chiba, Japan)

SSS27-P01 Room:Convention Hall Time:May 24 18:15-19:30

The stress distribution in the whole area of the slab changed completely after the 2004 off Kii Peninsula earthquake

MASE, Hirofumi[1*]

[1]none

(Please refer to the figure. Names of the slab, topography of seabed, etc are naming only of here.)

In (1), the relation between the 2004 off Kii Peninsula earthquake and the 1944 Tonankai earthquake was researched. Mantle that heads eastward in the Chugoku region pushes the edge of the Nankai slab. The slab is placed between the right-turning force and the reaction from the south of the Trough. There are two Seamounts that resist in the south of the Trough and the reaction-stresses concentrate in those. After the north side of the Seamounts was destroyed by the earthquake in 2004, the route that power is transmitted to the Seamounts converted from ”from North” to ”from Northwest”.

In (2), I searched for the evidence of the right-turn-force by using the focal mechanisms of earthquakes occurred on the surface of the Nankai slab and in it.

Because earthquakes that those compression axises and tangent of (circular arc)ar1-ar5 of which center of gyration is the south of Kii Suido harmonize are widely distributed, it turned out that power to induce the overall right-turn of the Nankai slab exists widely in each place.

I want to report on the result achieved by integrating (1) and (2).

The block arrows in Fig. 2 are average compression axial directions of the earthquakes that occurred in each area of the Nankai Slab obtained by (2). The compression powers to push the edge are transmitted in the slab and get to the Seamounts in which stress concentrate and to others. I expressed the typical transmission routes by A2,B2,C2,D2(arrows of short dashed line) following the block arrows. All except A2 are ”from North” compression routes connected directly with the Seamounts (Fig. 2). These routes converted those directions in 2004 in dramatic form. A2 and B2 were changed into A1 and B1 respectively and ”from Northwest” compression routes were formed (Fig. 1). Because the hypocenter of 1944 and 3 aftershocks were in a row and it was connected with WM Seamount (Fig. 1), it was able to be judged to be the compression route before 1944. The above is grounds of A1.

The outer of the right-rotation in 1944 traced the Crack(b) on inside from ar5 (4). Lateral-slip and collapse were generated because the transmission route until 1944 might have been C1,E1 (Fig. 1). Then, how did the transmission route after 1944 become? C1 curved to the west and changed into ”from North” compression route C2,D2. And, E1 changed into the compression power that turns eastward like E2 (Fig. 2). I think certainly so.

Observation facts of (6) do not contradict the existence of the compression power shown by E2 before the earthquake in 2004. And they harmonize with the hypothesis that E2 was changed into the compression power shown by E1 after the earthquake.

Expectation in the future is as follows. After ”from Northwest” compression continues for a while, the earthquake occurs and it returns to ”from North” compression. This is the next Tonankai earthquake. The earthquake in 2004 was a halfway mark. If it was a literal midway point, this cycle is 120 years, and the remaining time is 50 years.

(1)MASE/Two seamounts in the near south of Nankai Trough concentrate stress like stake/JpGU2015/S-SS30/abstract submission

(2)MASE/Focal mechanisms prove the right-turn of slab beneath Kii Peninsula/JpGU2015/S-SS31/abstract submission

(4)MASE(2014)/JpGU2014/SSS29-P10

(6)Suito,Ozawa(2006)/http://cais.gsi.go.jp/KAIHOU/report/kaihou77/12-1.pdf

SSS27-P01 Room:Convention Hall Time:May 24 18:15-19:30

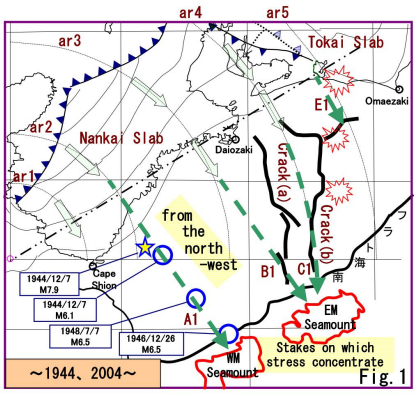

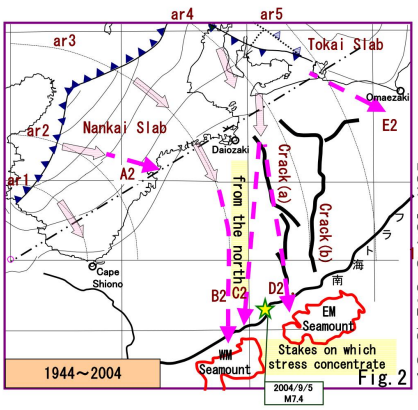

/About sea bottom
(shape line)
extracted from (7)/
/About "Nankai Slab"
(shape line, contour)
referable to (8)/
/About "Tokai Slab"
(shape line, contour)
referable to (9)/
/About information on earthquake
referable to (10)/

Reference literature
(5)木股・鷺谷(2005)/水準測量データの再検討による1994年東南海地震プレスリップ/名大
http://www.seis.nagoya-u.ac.jp/INTRO/report/jishinyochiren/162_kakegawa.pdf
(6)水藤・小沢(2006)/12-1GPS連続観測から見た東海スロースリップ/GSI
http://cais.gsi.go.jp/KAIHOU/report/kaihou77/12-1.pdf
(7)JHOD,JCG/Seafloor Topography of the Plate Boundaries
http://www1.kaiho.mlit.go.jp/jishin/sokuryo_E/sokuryo_E.html
(8)木村昌三(2001)/1946年南海地震に関係する四国における地震活動の特徴/(図2)
https://www.jstage.jst.go.jp/article/jgeography1889/110/4/110_4_581/_article/-char/ja/
(9)Nagoya Univ./Structure of the Subducting Philippine Sea Slab
http://www.seis.nagoya-u.ac.jp/SEIS/slab/slab-j.html
(10)JMA/Monthly Report on Earthquakes and Volcanoes in Japan/September 2004/特集2/図7-1(P65)
http://www.seisvol.kishou.go.jp/eq/gaikyo/index.html#monthly

Japan Geoscience Union Meeting 2015
(May 24th - 28th at Makuhari, Chiba, Japan)

SSS27-P02 Room:Convention Hall Time:May 24 18:15-19:30

Predicting earthquakes just before by observing electric fields

TAKAHASHI, Kozo[1*]

[1]None

The precursory seismic electric fields will be generated by the mechanism as follows:
(1) Before earthquakes, micro-cracks run in the source regions, and into these cracks pore water pours.
(2) Uranium compounds, radium compounds and radon, which exist in crystal boundaries, dissolve into the pore water.
(3) The cracks connect the pore water and spring water, and the radio active materials appear on the surface of source regions.
(4) The active materials ionize the lower atmosphere above the source regions, and the electric conductivity increases there locally and temporarily.
(5) The increase generates the current along the trace of cosmic shower between the surface and the ionosphere.
(6) As the current is intermitting and pulsating, it radiates wide band radio-waves, which are observed as the precursory waves.
The occurrence of the precursory micro-cracks of the item (1) is indispensable, but is not yet observed, though the radio active materials of (3), the cloud caused by the current of (5) and the wide band radio-waves of (6) are already observed before big earthquakes. So, the above mechanism will be appropriate.

2. Mechanism generating the current of item (5),
The top of thunderclouds has the voltage up to about 100 MV, so the electrons and negative ions flow into the clouds from the ionosphere. As a result, the ionosphere has a few MV. The mechanism, which increases the voltage at the cloud top, will be as follows (Refer to figs):
(I) At middle latitudes, water drops in cumulonimbus change into ice crystals in the area where the temperature is about -10 deg. The melting temperature of a solid is lower on the surface than the inside, so at about -10 deg. the ice crystals are covered with liquid water film. The inside of the crystals there are free electrons and positive holes, and the electrons can move to the surface water, but the holes can't. So the water film is negatively charged, and the solid part of crystals positively charged. In the cloud, the crystals collide with each other, the collision is approximately elastic one where lower than -10 deg., and the change of speed of the smaller crystals is bigger than that of larger ones. Then the negative charge in the surface film on the smaller crystals moves to the larger crystal, and the smaller crystals become smaller and charged positive, are blown up to the cloud top, and make it high voltage. On the other hand, the larger crystals become larger, negative and drop down on the ground.
(II) At low latitude, in the cloud no water crystal will exist, but upward electric fields of about 1 kv/m exist, as at other areas. So, water drops are polarized such as the top is negative and bottom is positive. When they collide, the negative charge in the top of smaller water drops, which have higher speed than the larger ones, neutralizes the positive charge in the bottom of the larger water drops, and the smaller ones become positively charged and are blown up to the cloud top, resulting the high voltage.
(III) In the smoke billowing from volcanos, the lightning is observed, where cinders, ashes and blocks collide with each other, and are charged by frictional electricity. By the same reason shown in (II), the charge is polarized and high voltage in the upper part of the smoke is generated. As this high voltage is observed, the explanation mentioned above will be valid.

3. Earthquake prediction by observing electric fields
The site where the earthquakes occur will be the place where the electric fields are observed, because the fields will be generated at the place where the micro cracks generated. The magnitude will be estimated from the size of the area where the fields generate, because the magnitude is about proportional to the size of the area. About to the occurrence time, about one week before big earthquake occurrence the fields started to be observed.

Keywords: earthquake prediction, precursory seismic slectric fields, mechanism of generating thunder, thunder in middle-latitude, thunder in low-latitude, thunder in smoke of volcano

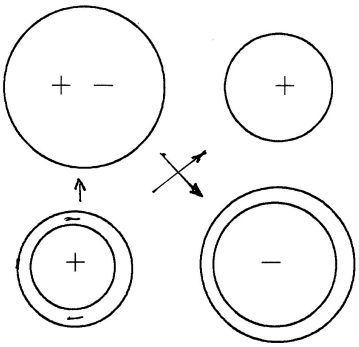

At middle latitude

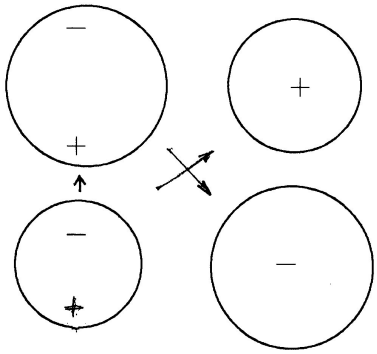

At low latitude

Japan Geoscience Union Meeting 2015
(May 24th - 28th at Makuhari, Chiba, Japan)

SSS27-P03 Room:Convention Hall Time:May 24 18:15-19:30

Long term predictability for the earthquake recurring a few times

TANAKA, Masayuki[1*] ; OKADA, Masami[1] ; UCHIDA, Naoki[2]

[1]Meteorological Research Institute, [2]Graduate School of Science Tohoku University

Sequential recurrent large/medium earthquakes listed in seismic catalog are not so many, usually considerably few due to long return period, which are available to calculate the long term probability. We study the predictability for those cases using 127 sequences of small interplate repeating earthquakes along the Japan Trench which have been applied for an experiment of prospective forecast. Two to five events closely preceding forecast are picked from each sequence to calculate the probabilities for qualifying event in 2008.

We use three models to calculate the probabilities, as follow:
(1) LN-Bayes: A Bayesian approach for lognormal distribution of recurrence interval with inverse gamma prior distribution.The parameters of inverse gamma are shape; phi=0.25, and scale; zeta=0.44.
(2) LN-SST: Lognormal distribution model base on the small sample theory.
(3) EXP-Pin: Exponential distribution model and the parameter being plugged in with the sample mean.

The ”Mean log-likelihood” and ”Brier score” mentioned below are used to score the forecast results.
Mean log-likelihood : Average of Ev∗log(P)+(1-Ev)∗log(1-P)
Brier score : Average of (P-Ev)ˆ2
Here P means forecast probability for event and Ev means presence (Ev=1) or absence (Ev=0) of the qualifying event. The model is considered to be superior to the alternative one, if the Mean log-likelihood is larger and Brier score is smaller than those of the alternative, respectively.

Keywords: recurrent earthquake, forecast, Bayesian approach, Small sample theory, Mean log-likelihood, Brier score

Japan Geoscience Union Meeting 2015
(May 24th - 28th at Makuhari, Chiba, Japan)

SSS27-P04 Room:Convention Hall Time:May 24 18:15-19:30

Seismic quiescence and activation that precede large earthquakes and their source regions

YOSHIKAWA, Sumio[1*] ; HAYASHIMOTO, Naoki[2] ; AKETAGAWA, Tamotsu[3]

[1]MRI, [2]MRI, [3]OMO

The authors have attempted to detect and to quantify the quiescence phenomena of seismic activity prior to large earthquakes, by using an analyzing method of seismic quiescence and activation (eMAP). They have shown that there are scaling laws of quiescent area and lead-time with respect to earthquake magnitude, which suggests the possibility of earthquake forecasting in intermediate time scales (Yoshikawa et al., 2014). As it is necessary to improve the accuracy for application of this method to the forecast, we have investigated in details the relationship between seismic quiescence and activation that precedes a large earthquake and the source region.

Our past investigation for 26 major earthquakes with the magnitude larger or equal to 6.7 (focal depths less than 200km) has shown that 15 cases of quiescence can be retrospectively detected before the earthquake, and revealed that there is a proportionality between the relative source distance (the distance from the rupture point to the center of quiet region) and the size of the quiescent area (the major axis). In the present study, we investigated the relationship between the source regions of earthquakes and the quiescent and activated areas for the above 15 cases. According to the result there were 12 cases where the seismically quiescent area is surrounded or neighbored by the seismically activated areas, which has been called as the doughnut pattern (Mogi, 1969). The result indicates that in most cases quiescence can be more easily identified by co-existence of the activated areas. In almost all cases the quiescent area did not fit to the whole source region of a future earthquake, but it overlaps only with a part of it. That is, the quiescent area does not determine the future source region. However, we could find that there are at least 9 cases where a source region overlapped with one of seismically activated areas when the doughnut pattern was formed. This possibly suggests that to detect the doughnut pattern can contribute to estimate a future earthquake source region.

As pointed by Mogi (1979), the first kind seismic gap is defined as an unbroken part to be considered as asperity in a seismic zone, whereas the second kind seismic gap is defined as a part of temporary seismic quiescence. That the seismic quiescent area described above does not fit to the whole source region means that seismic quiescence is not caused in the asperity but caused by decrease in seismic activity due to aseismic slip in the fault surface. On the other hand, the seismic activation in surrounding of the quiescent areas may be caused by seismic activity in asperity.

Keywords: seismicity, quiescence, earthquake forecast

Japan Geoscience Union Meeting 2015
(May 24th - 28th at Makuhari, Chiba, Japan)

SSS27-P05 Room:Convention Hall Time:May 24 18:15-19:30

On the witness testimonies before the 1946 Nankai earthquake on the Pacific coast of Kii peninsula, Japan

UMEDA, Yasuhiro[1*] ; ITABA, Satoshi[1]

[1]GSJ, AIST

On the coast area of Kii peninsula, the witness testimonies before the 1946 Nankai earthquake were examined by literature surveys. Reduced or muddy well water has been witnessed in 14 locations. Sea level change has been witnessed in three locations. Land subsidence has also been reported, but it may also post-seismic phenomenon of 1944 Nankai earthquake.

Keywords: 1946 Nankai earthquake, witness testimony, well water, sea level change, land subsidence

Japan Geoscience Union Meeting 2015
(May 24th - 28th at Makuhari, Chiba, Japan)

SSS27-P06 Room:Convention Hall Time:May 24 18:15-19:30

Relation between tidal triggering effect and interplate seismicity along the Tonga-Kermadec trench

HIROSE, Fuyuki[1*] ; KAMIGAICHI, Osamu[2] ; MAEDA, Kenji[1]

[1]Meteorological Research Institute, [2]Japan Meteorological Agency

Tonga-Kermadec Trench is one of the world's most earthquake-prone zone. A convergence rate of plate increases from the south to the north and in proportion to it, seismicity rate is increasing [Ide, 2013, Nature Geo.]. In this area, larger earthquakes with M>=7.5 including intraplate earthquakes have most occurred around 1980 and 2010 relatively. About the former period, it was pointed out that p-value (Schuster, 1897, PRSL, it's an index to express correlation between the seismicity and the tide. Generally when it is less than 0.05, judged to the correlation is high significant) was lowered before Tonga earthquake in December 1982 (Mw7.5) and increased after the mainshock by Tanaka, et al. [2002, GRL], using the GCMT data from 1977 to 2000. About the latter period, the interplate earthquake (Mw7.6) has occurred in March 2009 near the 1982 earthquake.

In this study, we investigate the temporal variation of p-value before and after the mainshock in 2009 by using the GCMT data whose end period was extended to 2013. We target interplate earthquakes in the global CMT catalogue (rake angle is 60-120 degrees, depth is 0-70 km, strike angle is 150-230 degrees, the periods is 1977-2013). Theoretical tidal response in the crust is expressed as summation of the earth tide and ocean tidal loading effect. The former is calculated by "earthtide_mod" [Ozawa, 1974; Nakai, 1979; Kamigaichi, 2015, personal com.], the latter is calculated by the modified program [Kamigaichi, 1998, PMG; Kamigaichi, 2015, personal com.] based on "Gotic2" [Matsumoto, et al., 2001]. These programs use the PREM as an earth model in order to calculate the green function and output the strain tensor at the hypocenter of each events [Kamigaichi, 2015, personal com.]. We calculate delta CFF with the frictional coefficient is 0.4 on the fault plane from the strain tensor obtained. We set 50 events as the calculation unit in order to estimate the temporal variation of p-value and shifted them at every 1 event. The results are as follows.

A. p-value decreases gradually before the 1982 mainshock and increases after that.

B. p-value decreases gradually (but at least 0.1) before the 2009 mainshock and increases after that.

C. There is five times of periods when p-value becomes less than 0.05 (Dec. 1982, Jan. 1988, Jun. 1993, Apr. 1998, Aug. 2000). However, about four times except for the mainshock in 1982, low p-value does not correspond large earthquakes with M>=7.0.

A p-value is expected be an important tool for earthquake forecast because p-value decreases before large earthquakes and increases after them (e.g., 2004 Off Sumatra earthquake (Mw9.0) and its largest aftershock (Mw8.6), and 2011 Off Tohoku earthquake (Mw9.0) [Tanaka, et al., 2010, 2012, GRL]). However, if we conduct the earthquake forecast using temporal changes of p-value, we must take into account the false alarm such as "item C" above mentioned.

Keywords: Earth tide, Ocean tidal loading effect, delta CFF, p-value, Tonga-Kermadec trench